Suboptimal Stochastic Control of a Continuous Latex Reactor

COSTAS KIPARISSIDES

Dept. of Chemical Engineering
Univ. of Alberta
Edmonton, Alberta, Canada

JOHN F. MacGREGOR
and
ARCHIE E. HAMIELEC

Dept. of Chemical Engineering
McMaster Univ.
Hamilton, Ontario, Canada

A suboptimal control algorithm is derived for a continuous latex reactor subject to deterministic and stochastic disturbances to control the pathological behavior of the reactor. An extended Kalman filter based on an instantaneous local linearization technique is used to estimate the reactor states, and a quadratic performance index is used to derive the suboptimal feedback control law. This study successfully demonstrates the application of the multivariable control theory to the control of a simulated continuous latex reactor operating under limit-cycle conditions. The mathematical model used for the control studies was previously developed and has been shown to describe the performance of an actual reactor system extremely well over its entire range of operation.

SCOPE

In the start-up of a latex CSTR, one usually observes an initial conversion overshoot followed by a long period of damped oscillations. Furthermore, in continuous emulsion polymerization the commercially important phenomena of sustained oscillations have been observed by several investigators. Experimental studies (Green et al., 1976, Kiparissides et al., 1978, 1980a) have shown that the conversion, number of polymer particles, and all other related properties often oscillate with time. In other words, a steady state is never achieved. It is evident that sustained oscillations and large start-up transient conversion overshoots are usually unacceptable; thus, control and start-up policies require investigation.

With the availability of modern process control computers, the practical implementation of advanced control theory in the polymer industries is certainly a reasonable possibility. However, before an advanced control strategy can be developed, a mathematical model of the process is required. Such a model for the continuous emulsion polymerization of vinyl acetate has been derived and tested extensively (Kiparissides et al., 1979, 1978). Moreover, an online technique has been developed that provides information about the model states from turbidity measurements (Kiparissides et al., 1980b).

In the present study, a suboptimal control algorithm is developed for a continuous latex reactor subject to deterministic and stochastic disturbances to achieve one or more of the following process objectives: (a) optimal start-up control of the reactor, (2) optimal change of operating production levels, or (3) regulator control to minimize the effects of process disturbances and of possible sustained oscillations.

CONCLUSIONS AND SIGNIFICANCE

The appearance of sustained oscillations in continuous latex reactors can lead to emulsifier levels too low to adequately cover polymer particles with the result that excessive particle agglomeration and reactor fouling might occur. Moreover, excursions to high polymer concentrations, due to the cycling behavior of conversion, may result in polymers with excessive branching and poor processability. Such a reactor operation is usually unacceptable, since it yields a product of varying quality.

In this study a control strategy is developed to improve the performance of a continuous latex reactor operating under sustained oscillation conditions. A multivariable stochastic control algorithm is derived that uses an instantaneous linearization technique to obtain a locally linear model from the nonlinear state equations that describe the continuous process. The linearized model is then integrated to give an equivalent discrete model. Noise models for the process and measurements are identified and a quadratic objective function is employed to derive the optimal feedback control law at each discrete control interval. An extended Kalman filter is used to obtain estimates of the state variables from online turbidity measurements.

To achieve our control objectives, a new reactor design is proposed that utilizes two additional streams of initiator and emulsifier as control variables. The multivariable control algorithm is then applied to a simulated continuous process. Simulation results show that continuous latex reactors can then be controlled to achieve a desired reactor performance. The new control policy enables us to greatly reduce sustained oscillations and large start-up transient conversion overshoots that usually appear in continuous latex reactors.

The successful application of the proposed control algorithm to the simulated continuous latex reactor should provide a good criterion of its value on the real process, since open-loop simulation studies were previously shown to represent experimental data collected from a lab-scale reactor.

0001-1541-81-4040-0013-$2.00.

LINEARIZED, DISCRETE STATE MODEL

When particle generation occurs only during certain periods of time and these periods of particle generation are sufficiently short, as in the case of reactor operation under sustained oscillations, the "*i*th" generation of particles in the reactor can be described by the following set of differential equations (Kiparissides et al., 1979, 1978):

$$\frac{dN_i(t)}{dt} = -\frac{N_i(t)}{\theta} + f(t) \tag{1}$$

$$\frac{dV_{pi}(t)}{dt} = -\frac{V_{pi}(t)}{\theta} + \frac{k_p d_m}{Nad_p}\,\phi(t)\,\bar{q}_i(t)\,N_i(t) \tag{2}$$

$$\frac{dx_i(t)}{dt} = -\frac{x_i(t)}{\theta} + \frac{k_p d_m}{M_T M_w}\,\phi(t)\,\bar{q}_i(t)\,N_i(t) \tag{3}$$

where N_i, V_{pi}, and x_i are, respectively, the number, polymer number, polymer volume, and conversion volume, and conversion of particles of the "*i*th" generation.

When two or more particle generations have appeared in the reactor, the total properties of the latex product at the exit of the reactor will be:

$$x(t) = \sum_{i=1}^{q_t} x_i(t);\ V_p(t) = \sum_{i=1}^{q_t} V_{pi}(t);$$

$$N(t) = \sum_{i=1}^{q_t} N_i(t) \tag{4}$$

where q_t denotes the number of discrete particle generations which have appeared in the reactor and is taken to be equal to one for steady state reactor operation (that is, continuous generation of particles). Eqs. 1 to 4 are highly coupled with the mass balance equations for initiator, emulsifier, monomer, and oligomeric radicals in the aqueous phase.

$$\frac{d[I]_w}{dt} = \frac{1}{\theta}([I]_F - [I]_w) - k_d[I]_w \tag{5}$$

$$\frac{d[S]_T}{dt} = \frac{1}{\theta}([S]_F - [S]_T) \tag{6}$$

$$\frac{d[M]_T}{dt} = \frac{1}{\theta}([M]_F - [M]_T) \tag{7}$$

$$\begin{aligned}\frac{d[R]_w}{dt} = \frac{1}{\theta}([R]_F - [R]_w) &+ 2fk_d[I]_w \\ &- k_{ab}A_p[R]_w k_v - k_m A_m[R]_w k_v - k_h[R]_w \\ &- k_{tw}[R]_w^2 + k_{de}N(t)\bar{q}(t)\end{aligned} \tag{8}$$

Symbols are defined in the notation. $\phi(t)$ is the monomer volume fraction in a particle and is given by:

$$\begin{aligned}\phi(t) &= \frac{1 - x(t)}{1 - x(t)\,(1 - d_m/d_p)}\,; \quad x > x_c \\ \phi(t) &= \phi_{\text{sat}}\,; \quad x \le x_c\end{aligned} \tag{9}$$

$\bar{q}(t)$ is the number of radicals per particle and is:

$$\bar{q}(t) = \left(\frac{2fk_d[I]_w}{2k_{de}\,N_i(t)} \cdot \frac{A_{pi}(t)}{A_p(t)}\right)^{1/2} \tag{10}$$

where $A_{pi}(t)$ is the surface area of the "*i*th" particle generation obtained from:

$$A_{pi}(t) = (36\,\pi)^{1/3}(\bar{v}_{pi}(t))^{2/3}\,N_i(t) \tag{11}$$

$f(t)$ represents the total rate for particle nucleation and it is given by:

$$f(t) = k_m A_m[R]_w k_v + k_h[R]_w \tag{12}$$

where A_m is the free coverage area of micelles given by:

$$A_m = [S]_T - S_{CMC} - A_p \tag{13}$$

The ability of this model to provide reactor simulations by specifying reactor operating conditions has been demonstrated through the simulation of experimental results of Green et al. (1976) and Kiparissides (1978) for both cases of limit-cycle and steady-state reactor operation (Kiparissides et al., 1979, 1978). Using experimental data obtained from a lab-scale latex reactor, the unknown kinetic parameters of the model have been estimated.

It is clear that the normal variational approach in which a nonlinear system is converted via Taylor series to a linear one cannot be easily employed for the linearization of the system of Eq. 1 to 4, especially when the reactor operates under limit-cycle conditions. Instead, we prefer to use a method proposed by Pearson (1962) and used successfully by Weber and Lapidus (1971), because as we shall see the nature of our nonlinear state equations is such that this procedure is much easier. The basis of this approach is the adoption of an instantaneously linearized time and state dependent model of the general form:

$$\begin{aligned}\dot{\underset{\sim}{x}} &= A(\underset{\sim}{x}, \underset{\sim}{u}, t)\underset{\sim}{x} + B(\underset{\sim}{x}, \underset{\sim}{u}, t)\underset{\sim}{u} \\ \underset{\sim}{x}(t_o) &= \underset{\sim}{c}\end{aligned} \tag{14}$$

$\underset{\sim}{x}$ and $\underset{\sim}{u}$ are the state and control vectors. A and B are general (nxn) and (nxr) system matrices found by estimation or mathematical linearization at a certain time. The selection of the coefficient matrices A and B is not unique and this method is clearly illustrated by Weber and Lapidus (1971). By providing instantaneous state and control values, the dependence of A and B on $\underset{\sim}{x}$ and $\underset{\sim}{u}$ can be eliminated to yield $A(t)$ and $B(t)$. Note that this form of system rearrangement merely transforms the equations so that if $\underset{\sim}{x}$ and $\underset{\sim}{u}$ are specified, the equations appear to be linear. Thus, we refer to it as an apparent linearization.

Since the reactor is to be controlled directly by a digital computer, it will be more convenient to have a corresponding discrete state space model. Thus, if the structure of A and B can be established by effectively factoring out $\underset{\sim}{x}$ and $\underset{\sim}{u}$ from the nonlinear system of Eqs. 1 to 4, a discrete system of equations can be obtained directly from the linearized continuous system (Eq. 14). By treating Eq. 14 as a piecewise constant coefficient equation, that is by approximating $A(\underset{\sim}{x}, \underset{\sim}{u}, t)$ and $B(\underset{\sim}{x}, \underset{\sim}{u}, t)$ with $A_k = A[\underset{\sim}{x}(k+1), \underset{\sim}{u}(k), kT]$ and $B_k = B[\underset{\sim}{x}(k+1), \underset{\sim}{u}(k), kT]$, it may be solved directly to give (Noton, 1972),

$$\underset{\sim}{x}(k+1) = \Phi(k+1, k)\,\underset{\sim}{x}(k) + \Delta(k+1, k)\,\underset{\sim}{u}(k) \tag{15}$$

where

$$\Phi(k+1, k) = \exp(A_k T) = \sum_{i=0}^{\infty} \frac{(A_k T)^i}{i!} \tag{16}$$

and

$$\Delta(k+1, k) = \int_o^T \exp[A_k(T - t)]\,B_k\,dt \tag{17}$$

where T is the discrete time interval equal to five minutes in our reactor studies. As expected, the method described is a function of the nonlinearity encountered but generally gives good correspondence. The linearization adopted has the advantage that a Lyapunov stability analysis can almost immediately be performed (Pearson, 1962).

The linearization and discretization methods described above can be applied to the reactor Eqs. 1 to 4. First, an instantaneously linear system is constructed in terms of the total properties. Then, a discrete model is derived by estimating $\Phi(k+1, k)$ and $\Delta(k+1, k)$ in terms of the A and B matrices.

The control variables, $\underset{\sim}{u}$, chosen for this study are the initiator and emulsifier concentrations in the reactor feed. Earlier open-loop simulation studies showed (Figures 1 and 2) that these variables could change the production level and reactor performance (oscillatory or steady state). They can in turn be changed by proper manipulation of the corresponding feed rates. A more detailed discussion on this subject is given later.

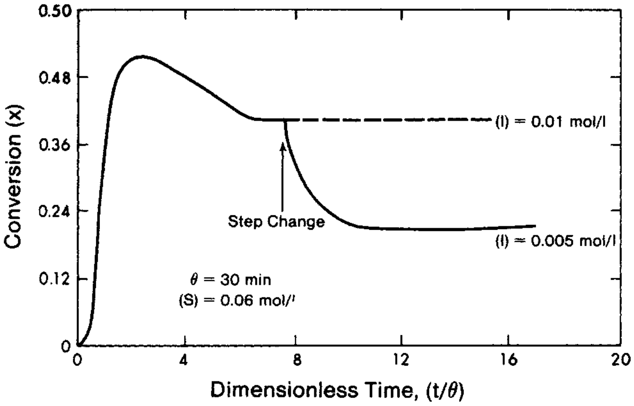

Figure 1. Effect of initiator concentration on the steady-state conversion level [(S) = 0.06 mol/L-H$_2$O; T = 50°C; M/W = 4/10].

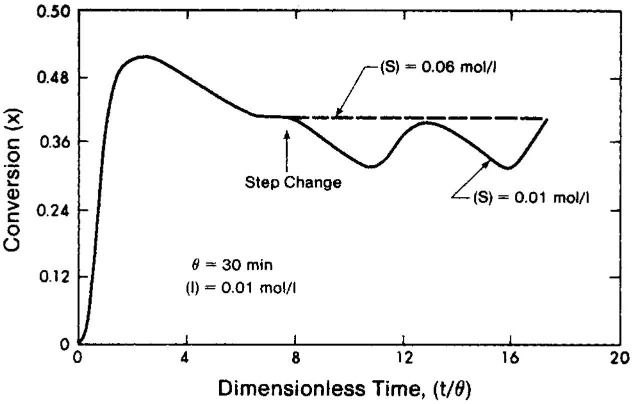

Figure 2. Effect of emulsifier concentration on reactor performance [(I) = 0.01 mol/L-H$_2$O; T = 50°C, M/W = 4/10].

Thus, the system of Eqs. 1 to 4 can be written:

$$\begin{bmatrix} \dot{N} \\ \dot{V}_p \\ \dot{x} \end{bmatrix} = \begin{bmatrix} -1/\theta & 0 & 0 \\ 0 & -1/\theta & 0 \\ 0 & 0 & -1/\theta \end{bmatrix} \begin{bmatrix} N \\ V_p \\ x \end{bmatrix} + \begin{bmatrix} B_{11} & B_{12} \\ B_{21} & B_{22} \\ B_{31} & B_{32} \end{bmatrix} \begin{bmatrix} I_F \\ S_F \end{bmatrix} \tag{18}$$

where

$$\begin{aligned} B_{11} &= f(t)/2I_F; & B_{12} &= f(t)/2S_F \\ B_{21} &= K_1\bar{q}N/2I_F; & B_{22} &= K_1\bar{q}N/2S_F \\ B_{31} &= K_2\bar{q}N/2I_F; & B_{32} &= K_2\bar{q}N/2S_F \\ K_1 &= \frac{k_p d_m \phi}{N a d_p}; & K_2 &= \frac{k_p d_m \phi}{M_T M_W} \end{aligned} \tag{19}$$

N, V_p, x, $\bar{q}$ are standing for the overall number of particles, polymer volume, conversion, and average number of radicals respectively and calculated by Eq. 4. Note that if there exist q_t generations of particles in the reactor at time t, one will actually have ($3 \times q_t$) differential equations of Eqs. 1 to 3 which must be combined using Eq. 4 in order to arrive at the total property balances (Eq. 18).

The corresponding constant matrices of the discrete system are:

$$\Phi(k+1, k) = [I_{33}]\, e^{-T/\theta} \tag{20}$$

$$\Delta(k+1, k) = \int_o^T e^{-(T-t)/\theta}\, dt\, B_k = \theta(1 - e^{-T/\theta})\, B_k \tag{21}$$

Note that the established structure for A and B matrices considerably facilitates the solution of Eqs. 16 and 17 to obtain the Φ and Δ matrices. Moreover, the parameters B_{ij} in Eq. 19 cannot be infinite, since the total initiator, I_F, and emulsifier, S_F, concentrations in the reactor feed are always different from zero. The last condition is a necessary one that the A and B matrices of the linearized system Eq. 14 should always satisfy. It should also be noted that in the above model the residence time θ is a function of the initiator and emulsifier feedrates used to control the reactor. Hence, it will vary from interval to interval in a stepwise manner.

EXTENDED KALMAN FILTER

The extended Kalman filter has been discussed in some detail by Jazwinski (1970) and only a brief discussion and the final equations will be given here.

The linear Kalman filter is an optimal estimator of the state vector $\underset{\sim}{x}$ (in a Bayesian or a minimum mean squared error sense) based on the information available at the current time y_t. If the observability conditions are satisfied, it is possible to obtain optimal estimates of unmeasured state variables. In the Kalman filter the current estimate of the state vector is a weighted sum of the prediction obtained from the model and information from new observations.

Consider the general nonlinear state equation:

$$\dot{\underset{\sim}{x}}(t) = f[\underset{\sim}{x}(t), \underset{\sim}{u}(t), t] \tag{22}$$

and suppose that at time t_{k+1}, it can be locally linearized (via Taylor series or via the procedure outlined above) about the current best estimates $\hat{\underset{\sim}{x}}(k+1/k)$ and the value of $\underset{\sim}{u}(k)$ over the past interval. That is, we have included the effects of the process and measurement noise vectors $\underset{\sim}{w}(k)$ and $\underset{\sim}{v}(k)$.

$$\begin{aligned} \underset{\sim}{x}(k+1) = {} & \Phi\,[\hat{\underset{\sim}{x}}(k+1/k), \underset{\sim}{u}(k), k]\,\underset{\sim}{x}(k) \\ & + \Delta[\hat{\underset{\sim}{x}}(k+1/k), \underset{\sim}{u}(k), k]\,\underset{\sim}{u}(k) + \underset{\sim}{w}(k) \end{aligned} \tag{23}$$

$$\underset{\sim}{y}(k) = H(k)\underset{\sim}{x}(k) + \underset{\sim}{v}(k) \tag{24}$$

where as before, $\underset{\sim}{x}(k)$ is an $(n \times 1)$ state vector, $\underset{\sim}{y}(k)$ is an $(m \times 1)$ vector of observed outputs and $\underset{\sim}{u}(k)$ is an $(r \times 1)$ vector of input variables. $\underset{\sim}{w}(k)$ and $\underset{\sim}{v}(k)$ are white Gaussian noise vectors with zero mean and covariances,

$$\begin{aligned} E\,[\underset{\sim}{w}(k)\underset{\sim}{w}'(k)] &= R_w \\ E\,[\underset{\sim}{w}(k)\underset{\sim}{v}'(j)] &= 0 \text{ for all } j \\ E\,[\underset{\sim}{v}(k)\underset{\sim}{v}'(k)] &= R_v \end{aligned}$$

In what follows the matrices Φ and Δ in Eq. 23 will, for convenience, be denoted by $\Phi(k+1, k)$ and $\Delta(k+1, k)$, their dependence on $\hat{\underset{\sim}{x}}(k+1/k)$ and $\underset{\sim}{u}(k)$ being understood.

For this model the filtered estimate of the state $\underset{\sim}{x}(k+1)$ given information up to and including $\underset{\sim}{y}(k+1)$ is given by:

$$\begin{aligned} \hat{\underset{\sim}{x}}(k+1/k+1) = {} & \hat{\underset{\sim}{x}}(k+1/k) + K(k+1)\,[\underset{\sim}{y}(k+1) \\ & - H(k+1)\,\hat{\underset{\sim}{x}}(k+1/k)] \end{aligned} \tag{25}$$

and the predicted estimate of the state $\hat{\underset{\sim}{x}}(k+1/k)$ based on information available at time t_k (used for the linearization above as well) is given by integrating the nonlinear state Eq. 22 from t_k to t_{k+1} with $\hat{\underset{\sim}{x}}(k/k)$ as initial conditions. That is,

$$\hat{\underset{\sim}{x}}(k+1/k) = \hat{\underset{\sim}{x}}(k/k) + \int_{t_k}^{t_{k+1}} f(\underset{\sim}{x}(t), \underset{\sim}{u}(t), t)\, dt \tag{26}$$

The approximate covariance matrices of these state estimates are given by:

$$\begin{aligned} P(k+1/k+1) = {} & P(k+1/k) \\ & - K(k+1)H(k+1)P(k+1/k) \end{aligned} \tag{27}$$

$P(k+1/k)$

$$= \Phi(k+1, k)P(k/k)\Phi'(k+1, k) + R_w \qquad (28)$$

The Kalman gain matrix $K(k+1)$ is given by:

$$K(k+1) = P(k+1/k)H'(k+1)$$
$$[H(k+1)P(k+1/k)H'(k+1) + R_v]^{-1} \qquad (29)$$

The steps involved in the practical implementation of the filter are summarized by Kiparissides (1978).

LINEAR-QUADRATIC STOCHASTIC FEEDBACK CONTROL

The design of constrained feedback controllers for linear, discrete, state space systems with constant coefficient matrices (Φ, Δ) is well known (Noton, 1972; MacGregor, 1973; Lapidus and Luus, 1967; Aström, 1970). Analytical solutions to the general problem are available for systems which can be formulated with a quadratic performance criterion. Consider the linear discrete state space equations:

$$\underset{\sim}{x}(k+1) = \Phi\underset{\sim}{x}(k) + \Delta\underset{\sim}{u}(k) + \underset{\sim}{w}(k) \qquad (30)$$

where Φ and Δ are time varying matrices. The linear-quadratic discrete control problem is defined here as that sequence of discrete control policies $\underset{\sim}{u}(k)$, $k = 0, 1, 2 \ldots N-1$ which minimizes the performance index:

$$J = E\left[\sum_{k=1}^{N}\{(\underset{\sim}{x}(k) - \underset{\sim}{x}^d)'Q(\underset{\sim}{x}(k) - \underset{\sim}{x}^d)\right.$$
$$\left. + (\underset{\sim}{u}(k-1) - \underset{\sim}{u}^d)'R(\underset{\sim}{u}(k-1) - \underset{\sim}{u}^d)\}\right] \qquad (31)$$

where Q and R are (nxn) and (rxr) symmetric nonnegative definite weighting matrices, and $\underset{\sim}{x}^d$ and $\underset{\sim}{u}^d$ are the desired final values of the state and control vectors, respectively.

Considering an augmented vector, $\underset{\sim}{z}$,

$$\underset{\sim}{z}(k) = (\underset{\sim}{x}(k), \underset{\sim}{x}^d, \underset{\sim}{u}^d)' \qquad (32)$$

the state Eq. 30 can be written in terms of the new vector $\underset{\sim}{z}$ as:

$$\underset{\sim}{z}(k+1) = \begin{bmatrix} \Phi(k+1, k) & 0_{33} & 0_{32} \\ 0_{33} & I_{33} & 0_{32} \\ 0_{23} & 0_{23} & I_{22} \end{bmatrix}\underset{\sim}{z}(k)$$
$$+ \begin{bmatrix} \Delta(k+1, k) \\ 0_{32} \\ 0_{22} \end{bmatrix}\underset{\sim}{u}(k) + \begin{bmatrix} I_{33} \\ 0_{33} \\ 0_{22} \end{bmatrix}\underset{\sim}{w}(k) \qquad (33)$$

or $\qquad \underset{\sim}{z}(k+1) = \Phi^*\underset{\sim}{z}(k) + \Delta^*\underset{\sim}{u}(k) + N^*\underset{\sim}{w}(k)$

where $\underset{\sim}{x}^d(k+1) = \underset{\sim}{x}^d(k)$; $\underset{\sim}{u}^d(k+1) = \underset{\sim}{u}^d(k)$ and I_{33}, I_{22} are identity matrices. The performance index (Eq. 31) can then be written:

$$J = E\,[\Sigma\{\underset{\sim}{z}'(k)Q_1\underset{\sim}{z}(k) + \underset{\sim}{u}'(k-1)Q_2\underset{\sim}{u}(k-1)$$
$$+ \underset{\sim}{z}'(k)V'\underset{\sim}{u}(k-1) + \underset{\sim}{u}'(k-1)V\underset{\sim}{z}'(k)\}] \qquad (34)$$

where Q_1 and Q_2 are symmetric positive definite matrices given as:

$$Q_1 = [I_{33}, -I_{33}, 0_{32}]'\ Q[I_{33}, -I_{33}, 0_{32}]$$
$$+ [0_{23}, 0_{23}, I_{22}]'\ R[0_{23}, 0_{23}, I_{22}] \qquad (35)$$

$$Q_2 = R \qquad\qquad V = R[0_{23}, 0_{23}, -I_{22}]$$

This quadratic performance criterion is quite general and the solution to this problem is given by the recursive set of matrix equations (Aström, 1970):

$$L(k) = [Q_2 + \Delta^{*\prime}(k, k-1)S(k+1)\Delta^*(k, k-1)]^{-1}$$
$$[V + \Delta^{*\prime}(k, k-1)S(k+1)\Phi^*(k, k-1)] \qquad (36)$$

$$S(k) = \Phi^{*\prime}(k, k-1)S(k+1)[\Phi^{*\prime}(k, k-1)$$
$$- \Delta^*(k, k-1)L(k)] - V'L(k) + Q_1 \qquad (37)$$

with initial $S(N) = Q_1$ and $k = N, N-1, \ldots, 1$. In these equations, $N = t_f/T$ *where* t_f is the final control time. The optimal feedback solution to this problem is given by:

$$\underset{\sim}{u}(k) = -L_\infty\hat{\underset{\sim}{z}}(k/\tau);\ N \to \infty \qquad (38)$$

where $\underset{\sim}{u}(k)$ is the optimal control setting to be applied at time t_k, and $\hat{\underset{\sim}{z}}(k/\tau)$ is the conditional expectation of the state vector $E[\underset{\sim}{z}(k)/\underset{\sim}{Y}(\tau)]$ *where* $\underset{\sim}{Y}'(\tau) = [\underset{\sim}{y}(\tau), \underset{\sim}{y}(\tau-1), \ldots, \underset{\sim}{y}(0)]$ represents the data available for determining the control action. L_∞ is a feedback control matrix given by the solution of recursive Eqs. 36 and 37. The state estimator $\hat{\underset{\sim}{z}}(k/\tau)$ can be obtained from the appropriate Kalman filter given previously.

This result implies that the optimal strategy can be separated into two parts: a state estimator for obtaining the best estimate of the state variables, and a linear feedback law which operates on the estimated state, both of which may be calculated independently of the other. This important result is referred to as the separation theorem or certainty equivalence principle, and results because we have assumed a linear system with Gaussian inputs at each point in time and have minimized a quadratic cost function.

In deriving Eqs. 33 to 38 in terms of augmented vector $\underset{\sim}{z}$, it was considered that our objective was to control the reactor so that a desired number of particles, polymer volume, and conversion, could be obtained. However, since it is more difficult to estimate the number of polymer particles at the present state of our online measurements, the problem of controlling the reactor to a certain desired conversion for given desired initiator and emulsifier concentrations is studied. Thus, the augmented vector $\underset{\sim}{z}$ and the Q_1, V' and R matrices will be:

$$\underset{\sim}{z}(k) = (\underset{\sim}{x}(k), x^d, I^d, S^d)'$$

$$Q_1 = \begin{bmatrix} q & 0 & 0 & -q & 0 & 0 \\ 0 & 0 & 0 & 0 & 0 & 0 \\ 0 & 0 & 0 & 0 & 0 & 0 \\ -q & 0 & 0 & q & 0 & 0 \\ 0 & 0 & 0 & 0 & r_1 & 0 \\ 0 & 0 & 0 & 0 & 0 & r_2 \end{bmatrix},\quad V' = \begin{bmatrix} 0 & 0 \\ 0 & 0 \\ 0 & 0 \\ 0 & 0 \\ -r_1 & 0 \\ 0 & -r_2 \end{bmatrix}$$

$$R = \begin{bmatrix} r_1 & 0 \\ 0 & r_2 \end{bmatrix} \qquad (39)$$

It is clear that before any further control analysis, the covariance matrices R_v and R_w as well as suitable values for the matrices Q and R should be determined. This is done next.

DETERMINATION OF R_w, R_v, Q AND R MATRICES

In a previous study (Kiparissides et al., 1980b) we showed how online turbidity measurements could be used to provide estimates of the model states. To relate the turbidity measurements to the model states, empirical regression models were derived that enabled us to predict the polymer volume and conversion at each sampling interval from a measurement of turbidity at seven different wavelengths. In order to extend the maximum amount of information from these turbidity measurements, a principal component analysis on turbidity values was used (Anderson, 1958). Thus, the measurement error $\underset{\sim}{v}(k)$ in Eq. 23 was approximated by the error vector $\underset{\sim}{e}$ resulting in fitting the model states to the turbidity measurements. We then choose the covariance matrix R_v to be:

$$R_v = \begin{bmatrix} \sigma_N^2 & 0 & 0 \\ 0 & \sigma_v^2 & 0 \\ 0 & 0 & \sigma_x^2 \end{bmatrix} = \begin{bmatrix} \mathrm{Var}(e_1) & 0 & 0 \\ 0 & \mathrm{Var}(e_2) & 0 \\ 0 & 0 & \mathrm{Var}(e_3) \end{bmatrix} \qquad (40)$$

To determine the filter gain matrix K from Eqs. 25 to 29, both R_v and R_w are required. $\underset{\sim}{w}(k)$ is often referred to as the "generation" noise and is difficult to interpret. For simplicity then (Jutan, 1976) it is assumed that $\underset{\sim}{w}(k)$ can be approximated by specifying a covariance matrix R_w as a diagonal matrix $R_w = \beta R_v$,

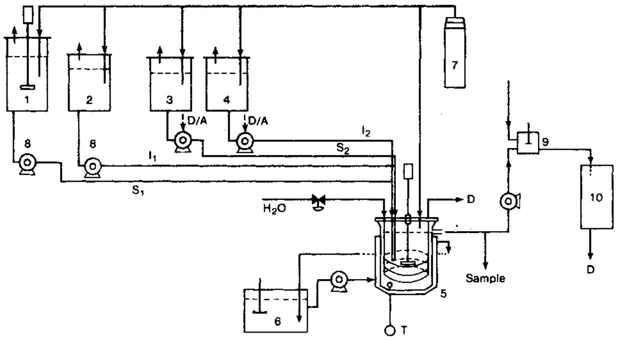

Figure 3. Schematic diagram of the proposed control system.

1, 2, 3, 4—Storage Tanks; 5—Reactor, 1.2L; 6—Constant Temperature Bath; 7—Nitrogen Supply; 8—Constant Flowrate Pumps, D/A-Variable Flowrate Pumps; 9—Dilution Vessel; 10—Spectrophotometer.

where β is a single parameter to be chosen. A similar idea was proposed by Hamilton et al. (1973) where the ratio between the diagonals of R_v and R_w determined the relative weight applied to the model against that applied to the measurements in the state estimation. A large ratio of R_v to R_w, as in this application, causes the model's contribution to be emphasized in the state estimate while a small ratio causes the data to be emphasized.

The quadratic performance criterion (Eq. 34) is quite general and includes the case of minimum mean square error control, that is Q = identity matrix, subject to a constraint matrix R, on the variance of the manipulated variables. Therefore, in Eq. 39, q will be equal to one. A satisfactory constraint matrix R may be chosen by calculating the variances of the outputs y and inputs u either analytically or by computer simulation. These variances should be jointly acceptable for a given R. For simplicity, R is chosen to be:

$$R = \begin{bmatrix} r_1 & 0 \\ 0 & r_2 \end{bmatrix}$$

and the parameters r_1, r_2 are varied until a satisfactory combination of input-output variances is obtained.

COMPUTER CONTROL OF A SIMULATED LATEX REACTOR

A computer algorithm has been developed to study the regulator control problem of a simulated latex reactor. This includes a routine which solves the nonlinear model, a routine for linearization and discretization, a Kalman filter, and a routine which computes the optimal initiator and emulsifier concentrations.

A schematic diagram of the proposed control system is shown in Figure 3. Two separate feeds are fed into the reactor at constant rate by an MPL-micro duplex pump. One feed stream contains the total amount of monomer, part of the recipe's total water and part of the emulsifier at a concentration, S_1.

The other feed contains an initiator solution of concentration, I_1. However, these constant flowrate streams (F_{1I}, F_{1S}) contain only a small amount of the total soap and initiator concentrations. The rest of the recipe's soap and initiator together with additional water are pumped through a set of two variable speed pumps. The flowrates of these two streams (F_{2I}, F_{2S}) are actually the two control variables. By varying the rpm of these two pumps, the total initiator or emulsifier concentration in the reactor feed can be changed.

The optimal initiator and emulsifier concentrations in the reactor feed can be obtained by adjusting the flowrates of the two variable control streams to satisfy the following mass balances:

$$F_{2I} = (F_T I_f^* - F_{1I} I_1)/I_2$$

$$F_{2S} = (F_T S_f^* - F_{1S} S_1)/S_2 \qquad (41)$$

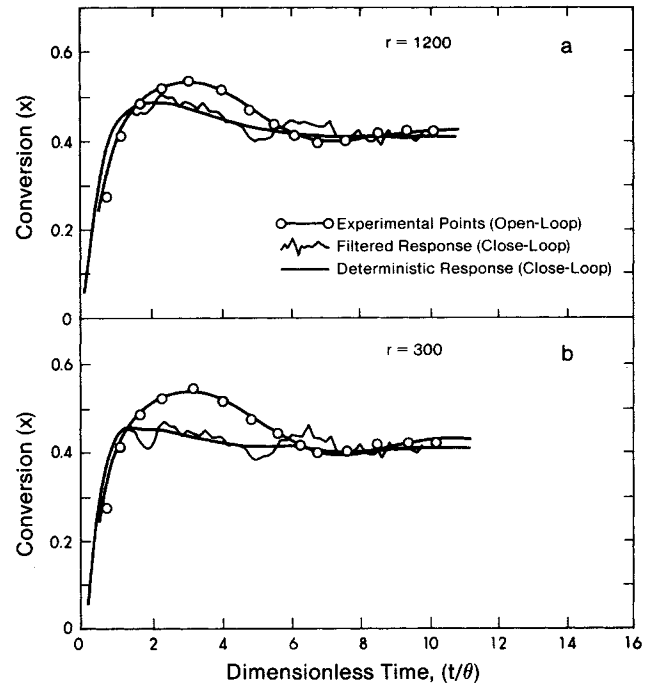

Figure 4. Start-up control: deterministic, filtered, and experimental (open-loop) conversion results for different values of parameter r [(I^d) = 0.01 mol/L-H_2O, (S^d) = 0.06 mol/L-H_2O, T = 50°C, M/W = 4/10].

where I_f^* and S_f^* are the optimal concentrations given by Eq. 38 and F_T is the total flowrate of water. However, because the concentrations of these two variable streams are very high (that is, $I_2 = 5I_1$, $S_2 = 10S_1$), small changes in the flowrates around their steady-state values can easily change the total initiator and emulsifier concentrations in the feed without unduly upsetting the mean residence time of the reactor. This is necessary, since large changes of the mean residence time can drive the reactor far from the desired conditions.

An alternative method would be to control the reaction temperature by manipulation of the coolant temperature. Thus, we could change the conversion by varying the temperature in the

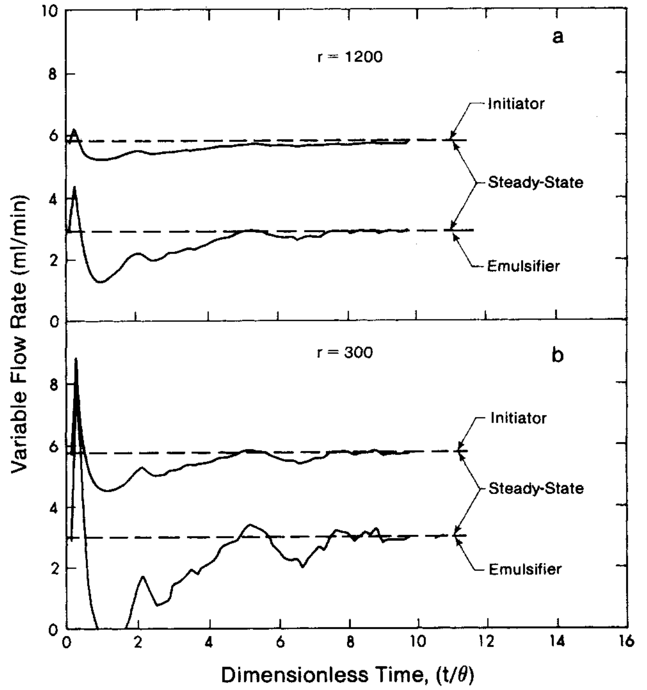

Figure 5. Start-up control: emulsifier and initiator variable feedrates vs. time [(I_1) = 0.0; (I_2) = 0.1 mol/L-H_2O; (S_1) = 0.022; (S_2) = 0.26 mol/L-H_2O].

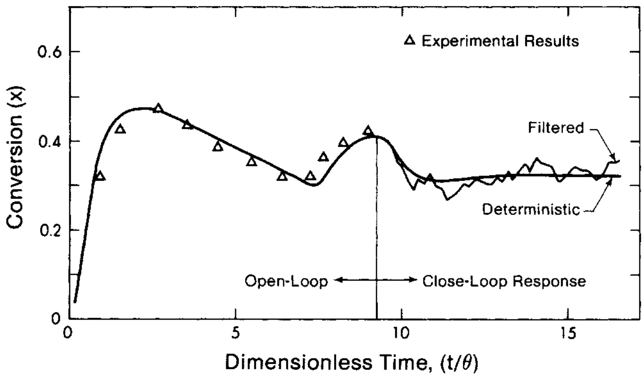

Figure 6. Control of sustained oscillations: conversion-time histories [$x^d = 0.36$; (I^d) = 0.01 mol/L-H_2O; (S^d) = 0.03 mol/L-H_2O; (I_1) = 0.0; (I_2) = 0.05 mol/L-H_2O; (S_1) = 0.018; (S_2) = 0.18 mol/L-H_2O].

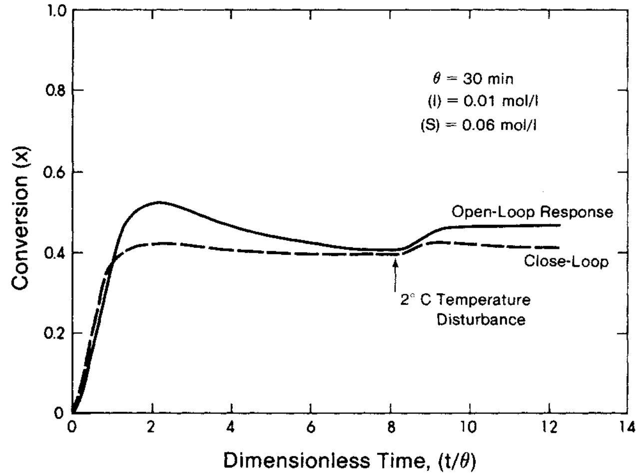

Figure 7. Control of temperature disturbances: conversion-time histories [$x^d = 0.40$; (I_1) = 0,0; (I_2) = 0.1 mol/L-H_2O; (S_1) = 0.022; (S_2) = 0.26 mol/L-H_2O].

reactor without upsetting the mean residence time of the reactor. Indeed, using the energy equation together with Eqs. 1 to 4, a suboptimal start-up policy was found that minimized conversion overshoot.

OPTIMAL START-UP CONTROL OF A LATEX REACTOR

Excursions into very high conversion regions and oscillatory behavior are usually unacceptable in commercial reactors; thus, optimal start-up control of a latex reactor is highly desirable. The numerical algorithm developed in the previous sections is applied to the problem of achieving steady-state conversion in such a way as to minimize the performance index (Eq. 34). Simulation results are shown in Figures 4 and 5.

In Figure 4, deterministic and filtered conversion responses are plotted against time for different values of constraint parameter, r. The desired steady state conversion value, x^d, was set equal to 40% and the desired emulsifier and initiator concentrations were $S^d = 0.06$ mol/L-H_2O and $I^d = 0.01$ mol/L-H_2O respectively. The constraint matrix R was chosen to be $R = rI_2$. A satisfactory constraint r was chosen by calculating the residual mean square deviations for the conversion output, and emulsifier and initiator inputs, u, and selecting a value which seemed to provide acceptable results. As the value of parameter r decreases (Figure 4), a faster output response is obtained as one would expect. For $r = 300$, a steady-state conversion value is achieved with very small overshoot (Figure 4b). By comparing the uncontrolled response (experimental results) with the controlled one (Figure 4b), it can be seen that a considerable reduction in start-up time and conversion overshoot has been achieved.

In Figure 5, the control variables (emulsifier and initiator flowrates) are plotted against time. It can be seen that the control variables deviate more from their corresponding steady state values as the constraint r decreases, which is expected since the constraints on the manipulated variables are relaxed. Large changes in the manipulated variables occur at the start of the polymerization and they are due to the initially large particle nucleation rates. It is clear from the results presented in this section that reactor overshoots and long reactor transients can be easily regulated by applying our suboptimal control algorithm to control the start-up of the reactor.

CONTROL OF REACTOR SUSTAINED OSCILLATIONS

For the online control of latex reactors, it would be desirable to attain specified steady-state values of conversion, to change in an optimal way the production level and to minimize the effects of process disturbances and eliminate oscillations in the production rate. A successful solution to these problems can largely improve the quality of the commercially produced latices with obvious economical advantages. In what follows, simulation results are presented which demonstrate the ability of the derived control algorithm to cope with the pathological behavior (sustained oscillations) and the effects of temperature disturbances often occurring in continuous emulsion reactors.

Figure 6 shows that the reactor is exhibiting sustained oscillations up to nine mean residence times. At that time a suboptimal control policy ($x^d = 0.36$, $I^d = 0.01$ mol/L-H_2O, $S^d = 0.03$mol/L-H_2O) is applied to the reactor that eliminates the oscillations and results in a steady state reactor behavior. Deterministic and filtered close-loop responses are plotted in Figure 6 as well as experimental results for the uncontrolled system. Note that the deterministic response does not attain its final value ($x^d = 0.36$), since the new increased emulsifier flowrate, F_{2S}, causes an actual decrease of the mean residence time and a subsequent decrease of conversion.

The effect of temperature disturbances on the steady-state conversion value is shown in Figure 7. The reactor has reached

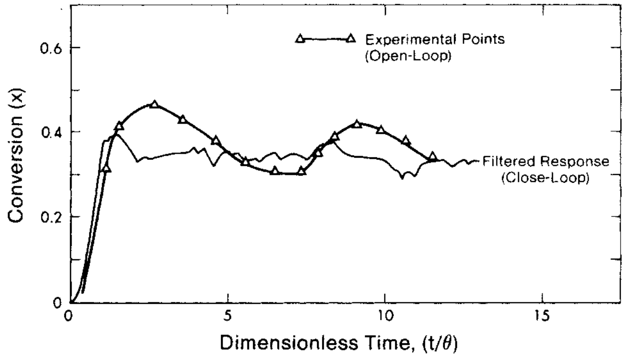

Figure 8. Control of sustained oscillations: conversion-time histories [$x^d = 0.36$; (I^d) = 0.01 mol/L-H_2O; (S^d) = 0.01 mol/L-H_2O].

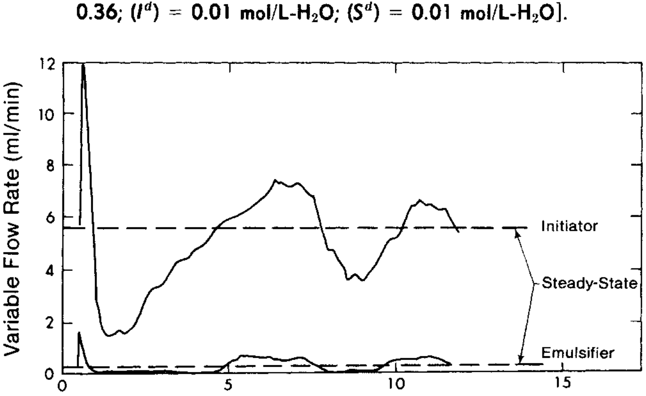

Figure 9. Emulsifier and initiator variable flow rates vs. time [(I_1) = 0; (I_2) = 0.05 mol/L-H_2O; (S_1) = 0.018; (S_2) = 0.18 mol/L-H_2O].

its final steady-state value ($x = 0.40$) when a step increase of the reaction temperature from 50 to 52°C forces the conversion to move to a new steady-state value ($x = 0.46$). However, when the reactor is controlled, the same temperature disturbance causes only a 1% increase in the conversion.

Figures 8 and 9 present simulation results for conversion and control variables. Regulatory control is applied to the reactor from the start of the reaction to eliminate sustained oscillations. The steady-state emulsifier concentration, S^d, is equal to 0.01 mol/L-H_2O and the corresponding initiator concentration, I^d, is 0.01 mol/L-H_2O. The steady-state mean residence time is 30 min. Experimental results show that under these constant input conditions, sustained oscillations will appear, Figure 8. To control this pathological behavior, a constraint matrix equal to

$$R = \begin{bmatrix} r_1 & 0 \\ 0 & r_2 \end{bmatrix} = \begin{bmatrix} 100 & 0 \\ 0 & 300 \end{bmatrix}$$

was used. Note that elimination of sustained oscillations is strongly affected by the proper choice of the constraint matrix, R. Figure 8 shows that the reactor attains an almost steady-state value ($x^d = 0.35$) and the magnitude of oscillations has been reduced. Under these new operating conditions, polymer particles are being generated during longer periods, approximately 30 min. compared with nucleation times of 2-5 min. observed for the uncontrollable process.

It is interesting to note in Figure 9 how the two variable feedrates change with time. During the time of particle nucleation, a large particle surface area is formed. This causes a large emulsifier deficit, since the coverage rate of particles by emulsifier exceeds the feed rate of fresh emulsifier to the reactor and results in a decrease of the particle nucleation rate. To prolong the particle generation and simultaneously increase the total particle growth rate, the flowrates of the control streams are increased. However, as conversion approaches its desired level, the variable feedrates start moving back to their corresponding steady-state values due to the effect of the constraint matrix R in Eq. 31. Figure 9 shows that the control variables have to follow a cyclic behavior to reduce the magnitude of oscillations in conversion.

NOTATION

A = (nxn) dynamic state matrix
A_m = total surface area of micelles, dm^2/L-latex
A_p = total surface area of polymer particles, dm^2/L-latex
B = (nxr) control matrix
d_m = density of monomer, g/L
d_p = density of polymer, g/L
fk_d = effective rate coefficient of initiator decomposition, s^{-1}
$f(t)$ = net rate of particle nucleation, l/s · L-latex
H = measurement matrix
I = initiator
$[I]_w$ = initiator concentration, mol/L-latex
$[I]_F$ = initiator concentration in the feed, mol/L-latex
I_m = m^{th} order unity matrix
k_{ab} = overall transport coefficient for radical transfer from the aqueous phase into polymer particles, dm/s
k_d = rate coefficient of initiator decomposition, s^{-1}
k_{de} = rate coefficient of radical escape from the polymer particles, s^{-1}
k_{fm} = rate coefficient of chain transfer to monomer, L/mol · s
k_h = rate coefficient of homogeneous nucleation, s^{-1}
k_m = rate coefficient of micellar nucleation, dm/s
k_p = rate coefficient of polymer propagation, L/mol · s
k_{tw} = rate coefficient of termination in aqueous phase
k_v = volume of emulsion phase over the volume of aqueous phase, L-latex/L
$[M]_F$ = monomer concentration in the feed, mol/L-latex
M_w = molecular weight of monomer
Na = Avogadro's number
$N(t)$ = total number of particles at t, 1/L-latex
$\overline{q}_i(t)$ = average number of radicals per particle of the i^{th} generation
q_t = number of discrete particle generations
$[R]_F$ = free radical concentration in the feed stream, mol/L-latex
$[R]_w$ = free radical concentration in the aqueous phase, mol/L-latex
R_w = variance covariance matrix for $\underset{\sim}{w}(k)$
R_v = variance covariance matrix for $\underset{\sim}{v}(k)$
$[S]_F$ = total emulsifier concentration in inflow, dm^2/L-latex
$[S]_T$ = total emulsifier concentration in the reactor, dm^2/L-latex
S_{CMC} = critical micelle concentration
T = sampling time, s
t = time, s
$\underset{\sim}{u}$ = vector of manipulated variables
V_p = total polymer volume, L/L-latex
$\bar{v}_{pi}$ = average polymer volume for a particle of the i^{th} generation
x_c = monomer conversion at which monomer droplets disappear, 20%
$x(t)$ = total monomer conversion
x_i = monomer conversion of the i^{th} generation of particles
$\underset{\sim}{x}$ = state vector
$\dot{\underset{\sim}{x}}$ = time derivative of state vector
$\hat{\underset{\sim}{x}}(k/k)$ = state estimate of $\underset{\sim}{x}$
$\underset{\sim}{y}$ = vector of output variables
$\underset{\sim}{z}$ = augmented state vector

$'$ = transpose of a matrix
$\sim$ = vector; e.g., $\underset{\sim}{w}$
$\hat{}$ = estimate; e.g., $\hat{\underset{\sim}{x}}(k/k)$
$\cdot$ = derivative with respect to time, e.g., $\dot{\underset{\sim}{x}}$
$E[\cdot]$ = expectation operator
d = desired value; e.g., I^d

LITERATURE CITED

Anderson, T. W., *An Introduction to Multivariate Statistical Analysis*, Wiley, N.Y. (1958).

Aström, K. J., *Introduction to Stochastic Control Theory*, Acad. Press, N.Y. (1970).

Greene, R. K., R. A. Gonzalez, and G. W. Poehlein, "Continuous Emulsion Polymerization—Steady State and Transient Experiments with Vinyl Acetate and Methyl Methacrylate," *Emulsion Polymerization*, eds, I. Piirma and J. L. Gardon, ACS Symposium Series **24**, 341 (1976).

Hamilton, J. C., D. E. Seborg, and D. G. Fisher, "An Experimental Evaluation of Kalman Filtering," *AIChE J.*, **5**, 901 (1973).

Jazwinski, A. H., *Stochastic Processes and Filtering Theory*, Acad. Press, N.Y. (1970).

Jutan, A., "State Space Modelling and Multivariable Stochastic Control of a Pilot Plant Packed-Bed Reactor," Ph.D. thesis, McMaster Univ., Hamilton, Ontario, (1976).

Kiparissides, C., "Modelling and Experimental Studies of a Continuous Emulsion Polymerization Reactor," Ph.D. thesis, McMaster Univ. Hamilton, Ontario (1978).

Kiparissides, C., J. F. MacGregor, and A. E. Hamielec, "Continuous Emulsion Polymerization Modelling Oscillations in Vinyl Acetate Polymerization," *J. Appl. Polym. Sci.*, **23**, 401 (1979).

Kiparissides, C., J. F. MacGregor, and A. E. Hamielec, "Continuous Emulsion Polymerization of Vinyl Acetate. Part I: Experimental Studies," *Can. J. Chem. Eng.*, **58**, 48 (1980a).

Kiparissides, C., J. F. MacGregor, and A. E. Hamielec, "Continuous Emulsion Polymerization of Vinyl Acetate. Part III: Detection of Reactor Performance by Turbidity-Spectra and Liquid Exclusion Chromatography," *Can. J. Chem. Eng.*, **58**, 65 (1980b).

Lapidus, L., and R. Luus, *Optimal Control of Engineering Processes*, Blaisdell Publishing Co., N.Y. (1967).

MacGregor, J. F., "Optimal Discrete Stochastic Control Theory for Process Applications," *Can. J. Chem. Eng.*, **51**, 468 (1973).
Noton, M., *Modern Control Theory*, Pergamon Press, N.Y. (1972).
Pearson, J. D., "Approximation Methods in Optimal Control. I: Suboptimal Control," *J. Electron. Control*, **13**, 453 (1962).
Weber, A. P. J., and L. Lapidus, "Suboptimal Control of Nonlinear Systems," *AIChE J.*, **17**, 3, 641 (1971).

Manuscript received August 20, 1979; revision received March 31, and accepted April 10, 1980.

Oscillatory States in the Oxidation of Carbon-Monoxide on Platinum

The trend observed on variation of the operating conditions during CO oxidation on platinum in a CSTR is as follows: stable states → simple oscillations → multipeak oscillations → stable states. Analysis of the experimental results indicates that a third or higher order system of differential equations is necessary to describe most of the observations.

M. SHEINTUCH

Dept. of Chemical Engineering,
Technion, Israel Institute of Technology,
Haifa, Israel

SCOPE

Self-sustained oscillatory states have been observed in several solid catalyzed oxidation reactions and have inspired several studies into the kinetics of these processes. The status of research into catalytic oscillations was reviewed by Sheintuch and Schmitz (1977) and by Slinko and Slinko (1978). The occurrence of isothermal oscillations seem to indicate that this behavior is caused by intrinsic kinetic rate processes. The interest in oscillatory catalytic reactions is due to the expectation that these studies will enhance our fundamental understanding of heterogeneous catalysis and that the knowledge of the mechanisms underlying this behavior will enable the assessment of the potential practical application of the phenomenon.

This paper presents a comprehensive account of oscillatory states in the oxidation of carbon monoxide on a Pt foil in a mixed reactor, in order to provide new insights into kinetic modeling of oscillatory catalytic reaction and to present new dynamic features of such states. The basic features of the cycle and the effect of flow rate have already been presented by Sheintuch and Schmitz (1977) and Plichta and Schmitz (1979); some intriguing and complicated phenomena such as multiplicity of limit cycles were presented by Sheintuch and Schmitz (1978). The analysis of the observations is qualitative only, in terms of basic principles and notions aimed at answering such questions as how many and what type of dynamic variables are required to explain the observations.

CONCLUSIONS AND SIGNIFICANCE

Three characteristic regimes exist in the oxidation of carbon-monoxide on platinum foil in a CSTR, as an operating variable (space velocity, feed concentration) is varied. At low CO concentrations and at large concentration the system is stable. At intermediate concentrations oscillatory states are observed. Two subregimes exist in the oscillatory regime: one where the oscillatory states are simple (one-peak-per-cycle), and a second where multipeak oscillations are observed. Several observations of multiplicity of oscillatory states and of nonstationary-aperiodic (termed chaotic) states are cited. Analysis of the uniformity of the features of the cycle revealed that deviations in the period, amplitude, and time average are small.

Analysis of the observations and experimental limit cycles presented in the plane of reaction rate vs. CO concentration indicates that: (a) the simplest system of differential equations necessary to describe the observations of simple oscillations is a second-order one accounting for two dynamic variables: a gas phase concentration and surface concentration; (b) a third or higher order system is necessary to describe the observations of multipeak oscillations, chaotic behavior, and the increase of the amplitude with that of space velocity.

EXPERIMENTAL SYSTEM

To avoid heat and mass transport resistances and the uncertain effects of dispersed crystallites, size and structure, the experiments were conducted with a Pt foil in a perfectly mixed (CSTR) gradientless reactor. An impeller rotating at 2,400 rpm provided a recirculating flow, forced upward in the annular area between the foil and the reactor wall, and downward through the inside of the cyclindrically shaped foil. The reactor walls, made of stainless steel (type 304) were coated with high-temperature aluminum point to avoid catalysis by the walls.

Two different foils, of 0.002 in thickness (obtained from Engelhard Ind.) and of 0.0025 in thickness (A. D. Mackay), were used in the course of this research. Both were of area 191 cm^2 and 99.995% purity. The feed consisted of 0-4% CO (CP grade), 10-20% oxygen (dry grade) and nitrogen (extradry grade). The pressure in the 460 cm^3 reactor was atmospheric and CO_2 concentration in the effluent stream was measured continuously using a CO_2 (infrared) analyzer.

A detailed description of the experimental system along with the pretreatment procedures which were applied are given by Plichta and Schmitz (1979). They have shown that while the gas phase temperature was time-invariant during the oscillations, the surface temperature oscillated with an amplitude of several degrees (<4°C).

0001-1541-81-4037-0020-$2.00. © The American Institute of Chemical Engineers, 1981.